ARCHIVES
of
FOUNDRY ENGINEERING

ISSN (2299-2944)
Volume 2025
Issue 4/2025

144 – 154

19/4

10.24425/afe.2025.157612

Published quarterly as the organ of the Foundry Commission of the Polish Academy of Sciences

Mechanical Performance of EN AC-Al Si12CuNiMg Alloy and Its SiC-Reinforced Composite Under Low-Temperature Conditions

K. Wacławiak, Abdisa Sisay Mekonnin *
Department of Materials Technologies, Faculty of Materials Engineering and Digitalization of Industry,
Silesian University of Technology, Krasińskiego 8, 40-019 Katowice, Poland
* Correspondence contact: e-mail: Abdisa.Sisay.Mekonnin@polsl.pl

Received 27.03.2025; accepted in revised form 16.06.2025; available online 31.12.2025

Abstract

This study investigates the mechanical properties of EN AC-AlSi12CuNiMg aluminium alloy (AlSi12) and its SiC-reinforced composite (AlSi12/10SiCp) under low-temperature conditions. Tensile tests were conducted at temperatures ranging from room temperature to -80°C using a testing machine equipped with a cooling chamber. The results reveal a significant temperature-dependent behaviour in both materials. As the temperature decreased, the ultimate tensile strength (UTS) of the AlSi12 alloy increased linearly from 140 MPa at room temperature to 194 MPa at -80°C, representing a 38.6% improvement. Similarly, the AlSi12/10SiCp composite exhibited a 15.3% increase in UTS, from around 170 MPa at room temperature to 196 MPa at -80°C. Both materials exhibited brittle fracture behaviour, with elongation values below 5% and no evidence of necking. Microstructural analysis using scanning electron microscopy (SEM) identified coarse grains, micro-pores, and intermetallic compounds as key factors degrading mechanical properties. Fractographic analysis revealed cleavage-like fracture surfaces with sharp morphologies and micro-cracks, consistent with brittle fracture modes. These findings highlight the limited ductility and enhanced strength of EN AC-AlSi12CuNiMg aluminium alloy and its composite at low temperatures.

Keywords: Cryogenic conditions, Mechanical properties, Fractography analysis, Microstructural characterization

Nomenclature

Al_2Cu	Aluminum Copper
Al_2O_3	Aluminium Oxide
AlN	Aluminium Nitride
AMCs	Aluminium Matrix Composites
°C	Degrees Celsius
EDS	Energy Dispersive X-ray Spectroscopy
FRASTA	Fracture Surface Topography Analysis
LNG	Liquid Natural Gas Carriers
LM	Light Microscope
Mg_2Si	Magnesium Silicide
MMCs	Metal Matrix Composites
MPa	Megapascal
SEM	Scanning Electron Microscope
SiC	Silicon Carbide
Si_3N_4	Silicon Nitride
TiB_2	Titanium Diboride
TiC	Titanium Carbide
UTS	Ultimate tensile strength
ZrB_2	Zirconium Diboride

1. Introduction

The demand for materials capable of withstanding very low temperatures or cryogenic temperatures is growing across diverse applications, such as liquid natural gas carriers (LNG) [1], aerospace [2], energy storage, military industries, cryogenic fuel tanks, hydrogen energy storage vessels, turbopumps, shipbuilding industries, etc. [3-5]. Ensuring the structural integrity and performance of materials under low-temperature conditions is critical for the safety and reliability of various technologies. This is particularly relevant for liquefied hydrogen storage tanks and cryo-compressed hydrogen storage at -253°C [3, 6], LNG carriers operating at approximately -163°C, and aircraft exposed to temperatures around -60°C at high altitudes [7]. In recent years, the study of the properties of metals for low-temperature applications has gained significant attention. Researchers worldwide have conducted extensive investigations in this domain. Published data indicate that a wide range of materials, such as aluminium alloys and composites, have been the focus of research efforts. Materials used in low-temperature applications are required to exhibit excellent mechanical properties, including a high strength-to-weight ratio, wear resistance, corrosion resistance, and the ability to withstand the ductile-to-brittle transition at very low temperatures [6, 9, 19]. These properties are critical to ensure structural integrity and reliable performance under extreme low-temperature conditions, where materials must maintain their toughness and resist brittle fracture.

Aluminium alloys are extensively utilized in low-temperature applications [10] due to their face-centered cubic crystal structure, which ensures high impact toughness and eliminates ductile-brittle transitions [11]. Their properties, including high strength, good processability, and resistance to hydrogen embrittlement, make them ideal for such low-temperature applications. As temperature decreases, the ultimate tensile strength (UTS), yield strength (YS), and elastic modulus of aluminium alloys typically increase, whereas elongation may vary depending on the specific alloy composition and microstructure [12, 13, 19]. Low-temperature aluminium alloys are categorized into solution-hardened types (e.g., Al–Mg 5000 series, Al–Mn 3000 series) and precipitation-hardened types (e.g., Al–Cu–Mg 2000 series, Al–Mg–Si 6000 series, Al–Zn–Mg 7000 series) [8, 19]. The use of aluminium alloys in engineering applications continues to expand in cold environments, as evidenced by their implementation in structures such as the Hålogaland Bridge in Norway, LNG storage tanks in Yancheng, Jiangsu Province, China, and the Deh Cho Bridge in Canada. Notably, 2219 aluminium alloy has been widely used in U.S. aerospace systems since the 1970s and continues to serve as a structural material for advanced rockets, including NASA's space launch systems and China's CZ-5 launch vehicles [14].

Different research studies have highlighted that aluminium alloys exhibit significant changes in mechanical properties at low temperatures, which are crucial for applications in cold environments. As the temperatures decrease, yield strength, ultimate tensile strength, and strain hardening rates generally increase, enhancing the alloys' performance. This response will explore the mechanical behaviour, deformation mechanisms, and practical applications of aluminium alloys at low temperatures. Yan et a. [15] conducted tensile tests on 6061-T6 aluminium alloy within a temperature range of 20 °C to −80 °C, demonstrating improvements in elastic modulus, yield strength, and ultimate tensile strength, while ductility remained largely unaffected. Also, Xi et al. [16] noted that a reduction in temperature from 20°C to -165°C improved the mechanical properties of AA 5083-H112 and 6061-T6 aluminium alloys. The study revealed an increase in elastic modulus, yield strength, and ultimate strength with reduced temperatures. Fracture strain decreased, and failure modes changed towards a more brittle nature in the test samples. Additionally, study in [14, 15], and [16] has demonstrated that aluminium alloys at low temperatures can enhance their strength.

In some application areas, conventional aluminium alloys are inadequate for low-temperature applications, particularly in the hydrogen energy sector, and structural elements subjected to very low temperatures are driving interest in advanced materials. In such cases, metal matrix composites (MMCs) with superior properties are necessary to meet these demands. Common reinforcements include cost-effective silicon carbide (SiC) [20] and aluminium oxide (Al_2O_3) due to their promising properties in harsh working environments. Other ceramic reinforcements, such as titanium carbide (TiC), aluminium nitride (AlN), silicon oxide (SiO_2), titanium diboride (TiB_2), silicon nitride (Si_3N_4), zirconium diboride (ZrB_2), and further enhance aluminium alloys [17, 18], [23, 24]. SiC particle-reinforced aluminium matrix composites are highly favoured for lightweight applications, offering enhanced strength, stiffness, creep resistance, and wear resistance compared to conventional aluminium alloys [25, 26].

Ozden et al. [27] investigated the impact behaviour of aluminium matrix composites (AMCs) reinforced with silicon carbide (SiC) particles at different temperatures. Their findings showed that factors such as particle clustering, particle cracking, and insufficient bonding between the aluminium matrix and SiC reinforcement play significant roles in determining the impact response of these composites, similar to studies [21, 22]. Notably, the study concluded that temperature variations exert minimal influence on the impact performance of AMCs. Aybarc et al. [28] reported that Al-metal matrix composites reinforced with SiC, Al_2O_3, and graphene show enhanced mechanical strength and low weight, making them ideal for high-performance applications. Also, Rong Li et al. [29] emphasised that the performance of aluminum composites with nanoscale reinforcements is primarily governed by the quality of interfacial bonding, identifying the bonding mechanisms, processing-related influences, and interface-optimization strategies as key factors in achieving high-performance composite materials. Ozben et al. [30] studied the mechanical properties of aluminium matrix composites (AMCs) reinforced with silicon carbide (SiC) particles. Their results demonstrated that increasing the reinforcement ratio enhanced the density of the composite, hardness, and tensile strength. Pawar et al. [31] investigated the mechanical properties of silicon carbide-reinforced aluminium matrix composites (AMCs) for use in power transmission components.

Fractography techniques, particularly SEM analysis, are essential for determining failure mechanisms through fracture surface examination, with a strong correlation observed between fractographic features and mechanical properties [32]. Methods such as the entire fracture surface method [33] and fracture surface topography analysis (FRASTA) [34] quantitatively correlate and thereby explain topographical details (e.g.,

roughness, crack propagation paths) with microstructural and loading conditions. These techniques are important for cryogenic applications where the brittle fracture modes dominate. FRASTA, for instance, reconstructs fracture progress by analysing the angles with which surfaces tilt and their roughness, giving insights into where failure initiated. The objective of this study is to evaluate the mechanical properties and examine how the EN AC-Al Si12CuNiMg alloy and its SiC-reinforced composite behave under low-temperature conditions, including detailed fractography analysis. To the authors best knowledge, no prior tensile tests have been conducted on cast samples of EN AC-AlSi12CuNiMg alloy or its SiC-reinforced composite under sub-zero temperatures, a key gap this study fills. While room/high-temperature data exist for similar alloys.

2. Experimental materials and methods

The studied materials were manufactured by the academic staff of the Department of Materials Technologies of Silesian University of Technology in Katowice and InnoMAT ltd. In this manuscript, the materials whose manufacturing process was described in papers [35] and [36] were used as test specimens. The chemical compositions of the EN AC-AlSi12CuNiMg alloy were presented in Table 1. For the composite, the EN AC-AlSi12CuNiMg alloy was used as the matrix material, and 10 wt% SiC particles were used as the reinforcement.

Table 1.
Chemical compositions of the EN AC-Al Si12CuNiMg aluminium alloy (wt%)

Fe	Si	Cu	Mg	Zn	Mn	Ti	Ni	Al
0.4	11.4	1.27	1.24	0.18	0.18	0.04	1.48	Rest

2.1. Mechanical tensile testing

A cylindrical specimen with a gauge length of 60 mm and a diameter of 10 mm (as shown in Figure1 (a) was utilized for experimental testing. Cryogenic tensile tests were conducted using a Z100 Zwick/Roell mechanical testing machine (illustrated in Figure 1b, equipped with a liquid nitrogen cooling chamber. The tests were performed at temperatures of -30°C, -60°C, and -80°C, under a strain rate of 0.0067 s^{-1}, based on ISO 6892-1:2016(E) maintained across all experiments. The selection of these parameter values was guided by insights from the literature, manufacturer recommendations, and established best practices. The liquid nitrogen gas-inlet flow was regulated via a magnetic valve. The strain rate was controlled by adjusting the displacement loading rate of the tensile apparatus. The used cooling chamber enables using traditional extensometers, which were at our disposal. We maintained the chamber temperature at a constant level for 30 minutes before testing to ensure the test specimen reached the predetermined set temperature. To ensure reproducibility, a minimum of three specimens were tested for each condition, and then the average values were recorded, with a total of 27 specimens evaluated overall. The specimens were subjected to uniaxial tensile loading until fracture, with load-elongation data recorded using the TestXpert software. Following the test, the fracture surfaces were examined using SEM.

2.2. Microstructure characterization

Microstructural analyses of both materials were conducted using scanning electron microscopy. The EN AC-AlSi12CuNiMg alloy and AlSi12/10SiCp composite were characterized using a scanning electron microscope (SEM) equipped with an X-ray spectrometer (VP S-3600N HITACHI, EDS from THERMO NORAN). Sample preparation adhered to standard metallographic protocols, beginning with polishing using waterproof silicon carbide papers up to 2000 grit. Final polishing was carried out with 3 μm and 1 μm diamond suspensions on a disc polisher, resulting in a mirror-like finish to enhance microstructural clarity.

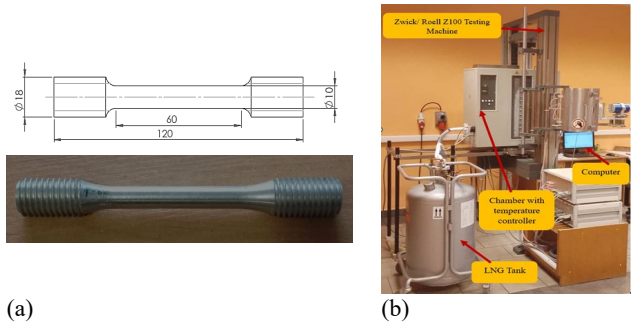

(a) (b)

Fig.1 Specimen geometry (dimensions in millimetres) (a), cryogenic tensile tests system (b)

3. Results and Discussion

3.1. Microstructure of EN AC-AlSi12CuNiMg alloy

The microstructural characteristics of the EN AC-AlSi12CuNiMg alloy prior to tensile testing were analysed using scanning electron microscopy (SEM) and light microscopy (LM), as shown in Figures 3(a) and 3(b), respectively. The microstructure predominantly consists of equiaxed grains with a homogeneous distribution. The chemical composition of the microstructural components in the AlSi12 alloy was determined through point analysis. Representative data, including EDS spectra and quantitative point analysis of the chemical composition of individual microstructural components, are also presented in Figure 2(a). The base AlSi12 eutectic alloy microstructure primarily comprises the primary α-Al phase, a

needle-like eutectic mixture of α-Al + β-Si (with proportions varying based on the Si content in the alloy), and polyhedral, plate-like primary Si crystals. Additionally, elements such as Cu, Mg, Ni, Mn, and Fe promote the formation of various intermetallic compounds. Identified intermetallic phases include Al_2Cu, Mg_2Si, and complex compounds within systems such as Al-Ni-Cu, Al-Fe-Si, and Al-Fe-Mn-Si. The morphology of the Si phases is subject to transformation due to modification and heat treatment processes. Additionally, the cooling rate plays a crucial role in determining the size, morphology, and distribution of the microstructural constituents, including intermetallic phases.

To determine chemical composition of microstructural components to necessary accuracy, point analysis was carried out, as illustrated in Figure 2(a). Representative EDS spectra and quantitative point analyses of the chemical composition for specific microstructural components of the alloys are shown in Figures 2(b) through 2(f).

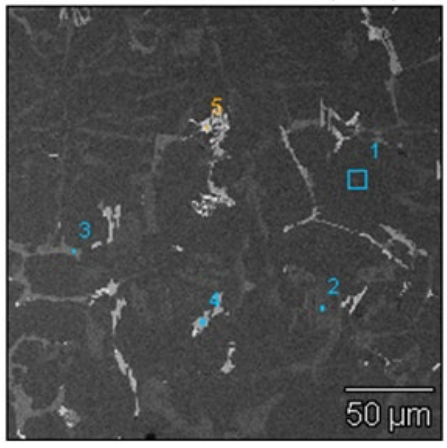

Weight %

	Mg-K	Al-K	Si-K	Cr-K	Mn-K	Fe-K	Ni-K	Cu-K
A(2)_pt1		98.4	1.6					
A(2)_pt2		14.4	85.6					
A(2)_pt3	10.2	33.8	29.7			9.4	16.9	
A(2)_pt4		42.1	6.4	1.0	12.4	27.8	5.1	5.3
A(2)_pt5		29.5	1.3			0.8	48.4	20.1

Fig. 2. (a). EN AC-AlSi12CuNiMg alloy with EDS point analysis showing elemental composition of microstructural components

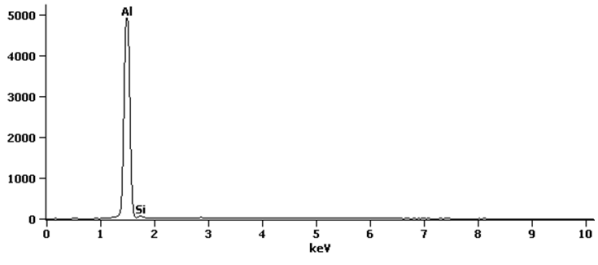

Fig. 2. (b). EDS diagram at point 1

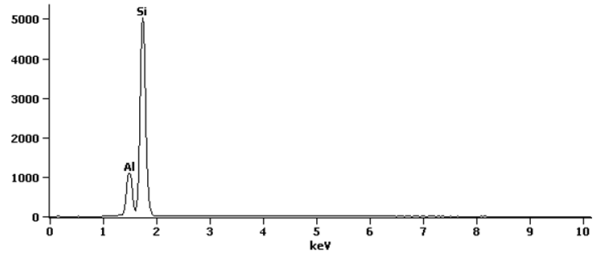

Fig. 2. (c). EDS diagram at point 2

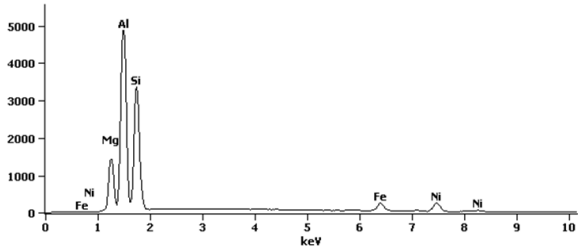

Fig. 2. (d). EDS diagram at point 3

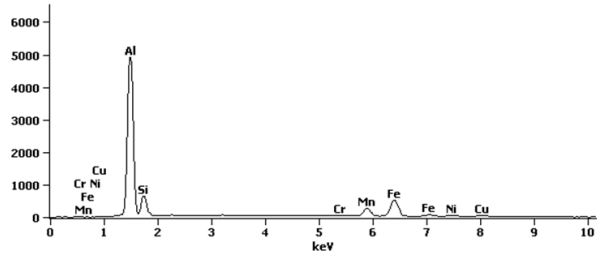

Fig. 2. (e). EDS diagram at point 4

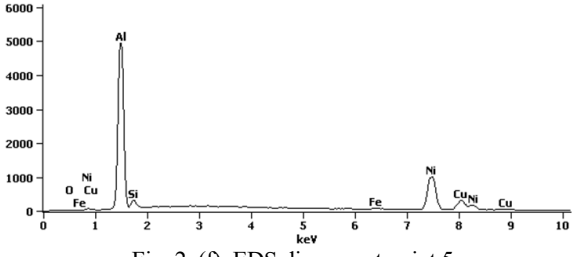

Fig. 2. (f). EDS diagram at point 5

The EDS analysis revealed a multiphase microstructure comprising a primary aluminium matrix, silicon-rich regions, and intermetallic compounds. Point 1 showed a dominant aluminium peak, confirming it as the aluminium-rich matrix. Point 2 exhibited a high silicon peak with minor aluminium, indicating a silicon-rich phase, likely primary or eutectic silicon. Point 3, as shown in the EDS spectrum, revealed prominent peaks for aluminium (Al) and silicon (Si), along with minor peaks for magnesium (Mg), iron (Fe), and nickel (Ni). This suggests that Point 3 lies at a transitional region between the aluminium matrix and a silicon-rich phase, possibly representing a eutectic Al–Si structure or an interfacial zone containing dispersed intermetallic compounds. Point 4 was dominated by aluminium, with detectable levels of Si, Ni, Cu, Cr, Mn, and Fe. The elemental combination suggests the presence of complex intermetallic

phases, potentially including Al–Fe–Ni or Al–Cu–Ni systems, which could influence the alloy's mechanical and thermal behaviour. The EDS analysis at Point 5 shows aluminium (Al) as the dominant element, indicating an Al-rich matrix. The presence of oxygen (O) suggests surface oxidation, likely forming Al_2O_3. Trace amounts of Fe, Cu, Ni, and Si were also detected.

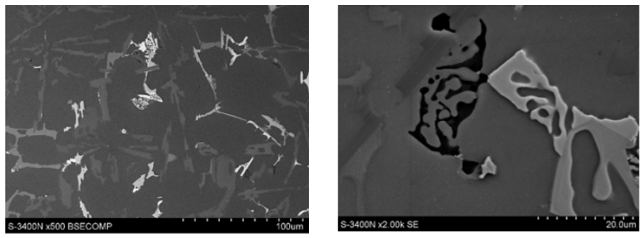

Fig.3. (a). Micrographs of the EN AC-AlSi12CuNiMg alloy captured at various magnifications using scanning electron microscopy (SEM)

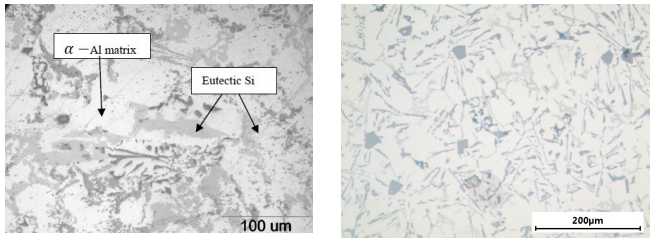

Fig. 3. (b). LM images of the EN AC-Al Si12CuNiMg alloy at different magnification [35]

3.2 Microstructure of the EN AC-Al Si12CuNiMg -10 wt% SiC composite

The microstructures of the EN AC-AlSi12CuNiMg/SiC composites are presented in Figures 4 and 5. The composite exhibited a multi-phase microstructure, comprising the aluminium matrix (Al), silicon (Si), and various intermetallic phases. The SiC reinforcement particles, visible as dark regions, were evenly distributed within the aluminium matrix. However, some porosity was observed near the reinforcement particles. The eutectic Si phase, which nucleated heterogeneously in a needle-like morphology on the surface of the SiC particles, is illustrated in Figures 4 and 5. The strong interfacial bonding between the SiC particles and the aluminium matrix, attributed to the formation of intermetallic compounds at the interface, is consistent with findings reported in the [16, 37]. Additionally, the incorporation of SiC particles led to significant grain refinement in the base alloy. This is evidenced by the finer grain size of the (Al) + (Si) eutectic structure compared to that of the unreinforced alloy.

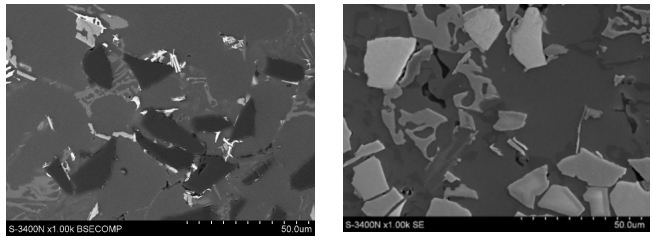

Fig. 4. SEM images of the EN AC-Al Si12CuNiMg/SiC composite at different magnifications

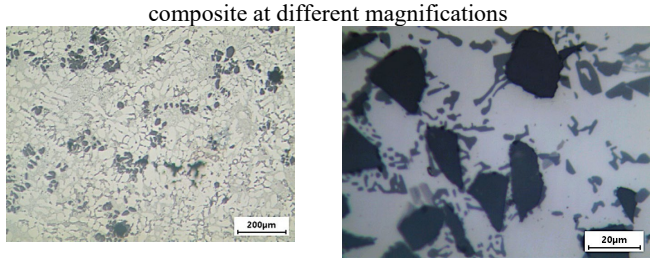

Fig. 5. LM images of the AlSi12CuNiMg/SiCp

3.3 Tension results and fracture state

The tensile strength, breaking strength, yield strength, and elastic modulus of materials can be obtained by the tensile test. To investigate the low-temperature mechanical properties of the EN AC-Al Si12CuNiMg alloy and SiC-reinforced composite, tensile tests were performed. At room temperature, the ultimate tensile strength of EN AC-Al Si12CuNiMg aluminium alloy and AlSi composite are 140 and 172 MPa, respectively. The tensile test at low temperature results (the average of minimum three tests, including ultimate tensile strength, breaking strength, and elongation, are summarized in Table 2 for the various test temperatures.

Table 2.
Tensile test results of EN AC-Al Si12CuNiMg aluminium alloy and Its SiC-reinforced composite at different temperature.

Materials	Temperature, °C (K)	Ultimate tensile strength, MPa	Breaking strength, MPa	Elongation, (%)
EN AC-Al Si12CuNiMg alloy	-80°C (193 K)	194	194	1.74
	-60°C (213 K)	173	173	2.08
	-30°C (243 K)	157	157	2.46
Reinforced studied alloy-composite	–80°C (193 K)	196	196	2.00
	-60°C (213 K)	192	192	2.20
	-30°C (243 K)	180	180	2.32

The ultimate tensile strength of the EN AC-AlSi12CuNiMg alloy increases with decreasing temperature, accompanied by a corresponding decrease in elongation, as illustrated in Figure 6 and Figure 7. This behaviour highlights the brittle nature of the

alloy under low-temperature conditions. Figure 7 shows the ultimate tensile strength of the EN AC-Al Si12CuNiMg alloy as a function of temperature. The values represent the average of three test results. The ultimate tensile strength exhibits an approximately linear increase, rising from 140 MPa at room temperature to 156 MPa at -30°C (243 K) and further to 194 MPa at -80°C (193 K), representing an improvement of approximately 38.6%, which aligns with Yan et al. [15], who reported a 10% improvement in ultimate tensile strength, and Jin et al. [10], who reported a 33% improvement in ultimate tensile strength of aluminium alloy. This trend is consistent with literature reports on aluminium-based alloys and composites, where cryogenic temperatures restrict dislocation motion, enhancing strength but reducing ductility. The observed improvement in strength aligns with findings reported in [38, 40] where similar behaviour was documented for aluminium alloys under cryogenic conditions.

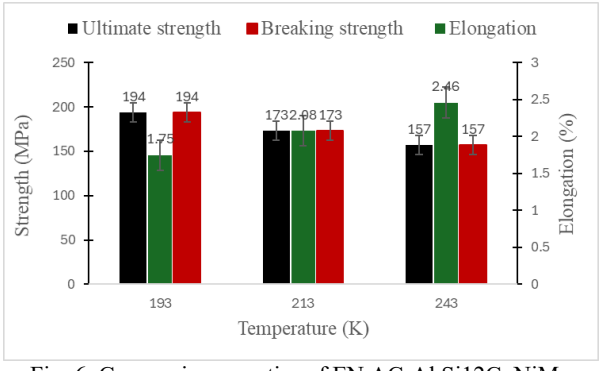

Fig. 6. Cryogenic properties of EN AC-Al Si12CuNiMg aluminium alloy at different temperatures

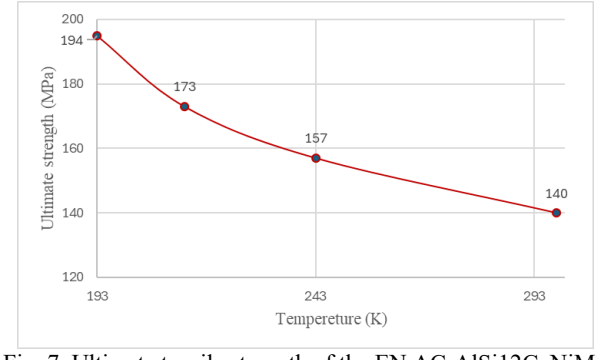

Fig. 7. Ultimate tensile strength of the EN AC-AlSi12CuNiMg alloy at various temperature

Similarly, as shown in Figure 8 and Figure 9, the AlSi reinforced with SiC shows an increase in strength from around 170 MPa at room temperature to 196 MPa at -80°C, representing a 15.3% improvement, aligns with Jin et al [10]. This lower percentage increase compared to the EN AC-Al Si12CuNiMg alloy can be attributed to the already elevated strength of the composite at room temperature due to the reinforcing effect of SiC particles. The SiC reinforcement enhances strength through mechanisms such as load transfer and dislocation pinning, but the relative improvement at cryogenic temperatures is less pronounced because the composite starts with a higher baseline strength [39, 40].

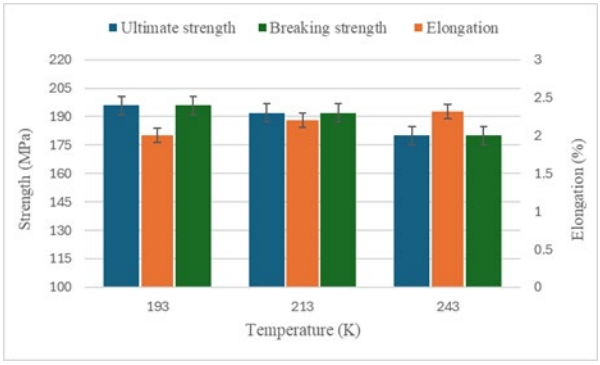

Fig.8. Cryogenic properties of the AlSi reinforced with SiC at different temperature.

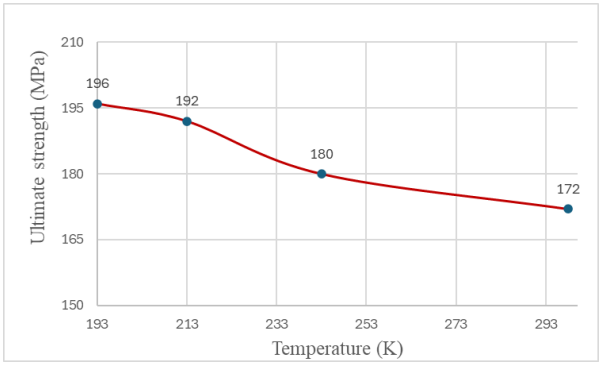

Fig.9. Ultimate tensile strength of the AlSi reinforced with SiC at various temperature

Throughout the tested temperature range, both materials exhibit low elongation values (<5%), indicating limited ductility. The breaking strength closely matches the ultimate tensile strength as illustrated in figure 6 and 8, confirming failure at maximum stress without plastic deformation as in Figure 10. Fractographic analysis shows no necking or distortion near the fracture zone, with sharp, intact fracture edges, characteristic of brittle failure. Additionally, the absence of distinct yield strength suggests no plastic deformation under loading. These findings align with previous studies in [16] on aluminium alloys and composites at cryogenic temperature. The observed brittle behaviour highlights the need for careful consideration in low-temperature applications where ductile-brittle transition resistance is critical. This trade-off between strength and ductility is a well-documented phenomenon in cryogenic materials science. For instance, studies on aluminium-silicon alloys reinforced with SiC particles have shown that while the reinforcement enhances strength, it can also exacerbate brittleness at low temperatures due to stress concentration effect. These findings emphasize the importance of optimizing material microstructure, such as SiC particle distribution and size, to mitigate brittle failure in demanding environments. In addition to the temperature-dependent strength and ductility behaviour, it is important to consider the effect of

microstructural changes on the material's performance. At lower temperatures, the EN AC-Al Si12CuNiMg alloy experiences a reduction in atomic mobility, which influences the precipitate hardening mechanisms. The increased dislocation pinning at lower temperatures impedes dislocation motion, contributing to the observed strength increase but also leading to a loss in ductility [27]. This behaviour is further affected by the alloy's specific phase composition, particularly the formation and distribution of intermetallic compounds, which can become more brittle at cryogenic temperatures. Understanding the relationship between the alloy's microstructure and its mechanical properties at low temperatures is crucial for optimizing its performance in cold environments, especially when dealing with components subjected to very low temperatures.

The results of the study indicate that the EN AC-AlSi12CuNiMg alloy and SiC reinforced AlSi composite both exhibit an increase in ultimate tensile strength as the temperature decreases at low temperatures (-30, -60 and -80°C). At these temperatures, the materials experience brittle fracture, reports failure mode without yielding. On the other hand, at elevated temperatures (150, 200, 250, 300 and 350°C), the materials indicated the opposite behaviour. According to studies presented in papers [34, 35], both materials experience a reduction in ultimate tensile strength and yield strength with increasing temperature.

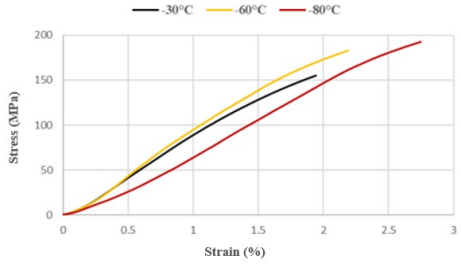

Fig. 10. Stress-strain behaviour of EN AC-Al Si12CuNiMg alloy at different temperature

Young's modulus, which quantifies a material's resistance to axial deformation, is determined from the slope of the axial stress-strain curve. This property is temperature-dependent, as illustrated in Figures 11, which show the relationship between temperature and Young's modulus for the EN AC-AlSi12CuNiMg alloy and its SiC-reinforced composite. The mean Young's modulus, calculated from three experimental measurements, was plotted over different test temperature, with the room temperature value included for reference. The results demonstrate that the Young's modulus of both materials increases at lower temperatures. However, it should be noted that the measurements have some degree of uncertainty, as elongation was not recorded using a high-precision extensometer but was instead based on the crosshead displacement.

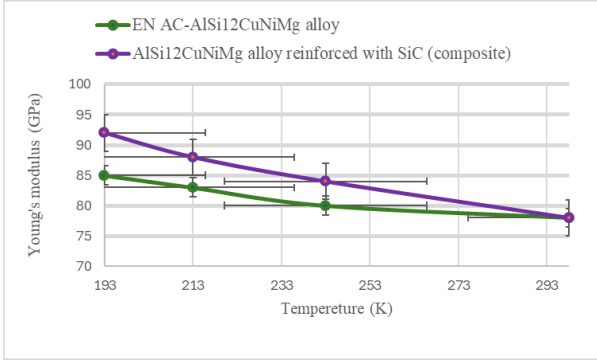

Fig. 11. Temperature dependence of Young's modulus for the EN AC-AlSi12CuNiMg alloy and its SiC-reinforced composite

3.4 Fractographic SEM observations

Fractographic analysis of the samples at -30°C, -60°C, and 80°C consistently revealed a transcrystalline fracture mode, characterized by sharp and intact morphologies on the fracture surfaces. Remarkably, the absence of the typical ductile cup and cone pattern further confirms the brittle fracture nature of the α-Al matrix and the eutectic Si phases in the cast aluminium alloy under low temperature tensile testing. The smooth and featureless fracture surfaces imply minimal plastic deformation prior to failure, which is a hallmark of brittle fracture mechanisms. Brittle fracture in materials is often defined by its rapid propagation with little energy absorption, and it typically follows cleavage or intergranular paths.

Fig. 12. Failure state of EN AC-Al Si12CuNiMg aluminium alloy at different low-temperature

The fracture surfaces of EN AC-Al Si12CuNiMg alloy and AlSi composite reinforced with SiC, tested at -30°C, -60°C, and -80°C, exhibited distinct brittle characteristics. Shiny, granular regions, flat surfaces, and sharp edges indicated brittle crack propagation. Conchoidal patterns, chevron markings, and radial lines traced crack initiation from stress concentrators like eutectic Si and intermetallic phases. Hackle marks, river patterns, and cleavage facets confirmed brittleness, while step-like features and intergranular textures highlighted weak interfaces. The sharpness of silicon particles and intermetallic phases suppressed plastic deformation, intensifying brittleness under tensile loads. Figure 13 (5 mm–200 μm) illustrates these effects.

The macroscopic fractography indicate that the initial crack originated at the edges of the samples, as observed at a lower magnification of 5 mm and the macroscopic image highlights distinct zones, as in Figure 13. The final fracture of the specimen exhibits cleavage, characterized by flat and faceted features, which are indicative of brittle fracture. This brittle behaviour is evident in the fracture structure and is further confirmed by the flattened crack progression. The presence of a flat surface signifies the dominance of brittle fracture, primarily attributed to the cryogenic treatment applied during testing.

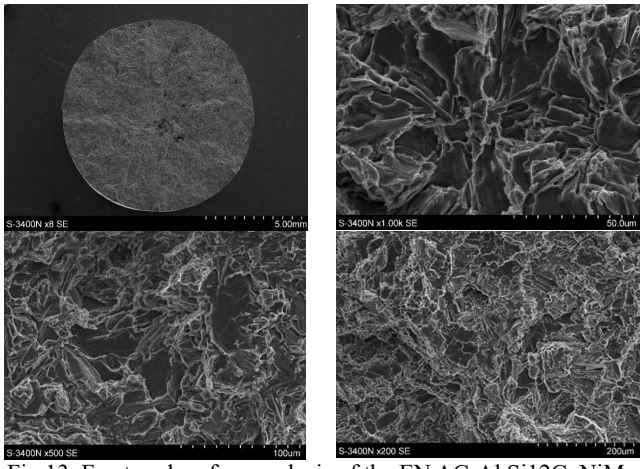

Fig.13. Fractured surface analysis of the EN AC-Al Si12CuNiMg alloy

The fractographic analysis of the EN AC-Al Si12CuNiMg alloy tested at -60°C, conducted using a scanning electron microscope reveals distinct brittle fracture characteristics. At the highest resolution (50 µm), the fracture surface displays sharp cleavage facets, flat regions, and hackle marks, which are indicative of trans granular brittle fracture. Radial markings and localized crack propagation paths are observed, originating from stress concentrators such as eutectic silicon particles and intermetallic phases. These features highlight the initiation and propagation mechanisms driven by microstructural inhomogeneities. The lack of plastic deformation in this region emphasizes the brittle nature of the fracture.

At a 100 µm scale, the fracture surface exhibits granular textures and conchoidal fracture patterns, further confirming brittle failure mechanisms. Chevron markings are evident and trace the origins and growth directions of cracks under tensile stress. These features demonstrate the role of silicon particles and intermetallic phases as primary stress concentrators, which govern crack nucleation and propagation in the brittle regime. This magnification provides an intermediate view, linking the finer details at higher resolution to the macroscopic features visible at lower magnifications.

At a 200 µm scale, the fracture surface reveals step-like features, river patterns, and intergranular textures, characteristic of brittle cleavage fracture. Weak interfaces in the microstructure, such as grain boundaries or matrix-reinforcement interfaces, act as preferred paths for crack propagation. Shiny, reflective regions associated with sharp silicon particles and intermetallic phases emphasize their role in enhancing crack propagation and brittleness. The global fracture morphology observed at this scale corroborates the influence of microstructural features on brittle fracture behaviour at low temperatures.

Overall, fractographic analysis at all magnifications confirms brittle fracture at -30°C, -60°C, and -80°C characterized by cleavage facets, radial patterns, hackle marks, and intergranular features. The sharp eutectic silicon particles and intermetallic phases suppress plastic deformation, increasing brittleness, while weak interfaces promote intergranular fracture. The further suppression of plasticity at sub-zero temperatures exacerbates brittleness, highlighting the need to mitigate these microstructural weaknesses to enhance the alloy's performance in low-temperature applications.

The fractographic analysis of the failed composite specimen was performed using SEM at 5 mm, 50, 100 and 200 µm resolutions to investigate the underlying failure mechanisms as in Figure 14. Tensile testing revealed fracture without significant necking, with the ultimate tensile strength (UTS) equalling the breaking strength, suggesting a predominantly brittle failure mode. Microstructural examination further confirms this, highlighting features characteristic of trans granular cleavage fracture and radial crack propagation, indicative of rapid crack advancement with minimal plastic deformation. Key brittle fracture features include cleavage facets with well-defined, flat fracture planes, confirming crack propagation along crystallographic paths. Radial crack progression and the presence of secondary cracks further suggest a stress-driven failure mechanism, characteristic of low-energy fractures in brittle materials. These observations indicate that the material primarily failed through brittle cleavage fracture, driven by high stress concentrations and limited energy absorption.

Additionally, porosity defects observed in the composite act as stress concentrators, accelerating crack initiation and propagation. The presence of SiC-matrix debonding at various regions further highlights weak interfacial bonding, reducing load transfer efficiency and compromising mechanical integrity. The interplay of brittle cleavage, flat faces, secondary cracking, and interfacial debonding suggests a mixed fracture mechanism, where localized plasticity is insufficient to prevent predominant brittle failure, likely influenced by thermal or mechanical stress conditions.

The correlation between mechanical testing data and fractographic observations confirms a brittle-dominant failure mechanism, with cleavage and secondary cracking as primary modes. The presence of minor ductile features indicates a mixed-mode failure, warranting further high-magnification SEM imaging, electron backscatter diffraction (EBSD), and energy-dispersive X-ray spectroscopy (EDS) to assess microstructural effects on crack propagation. These findings are crucial for optimizing fracture resistance, failure mitigation, and composite processing strategies in structural applications.

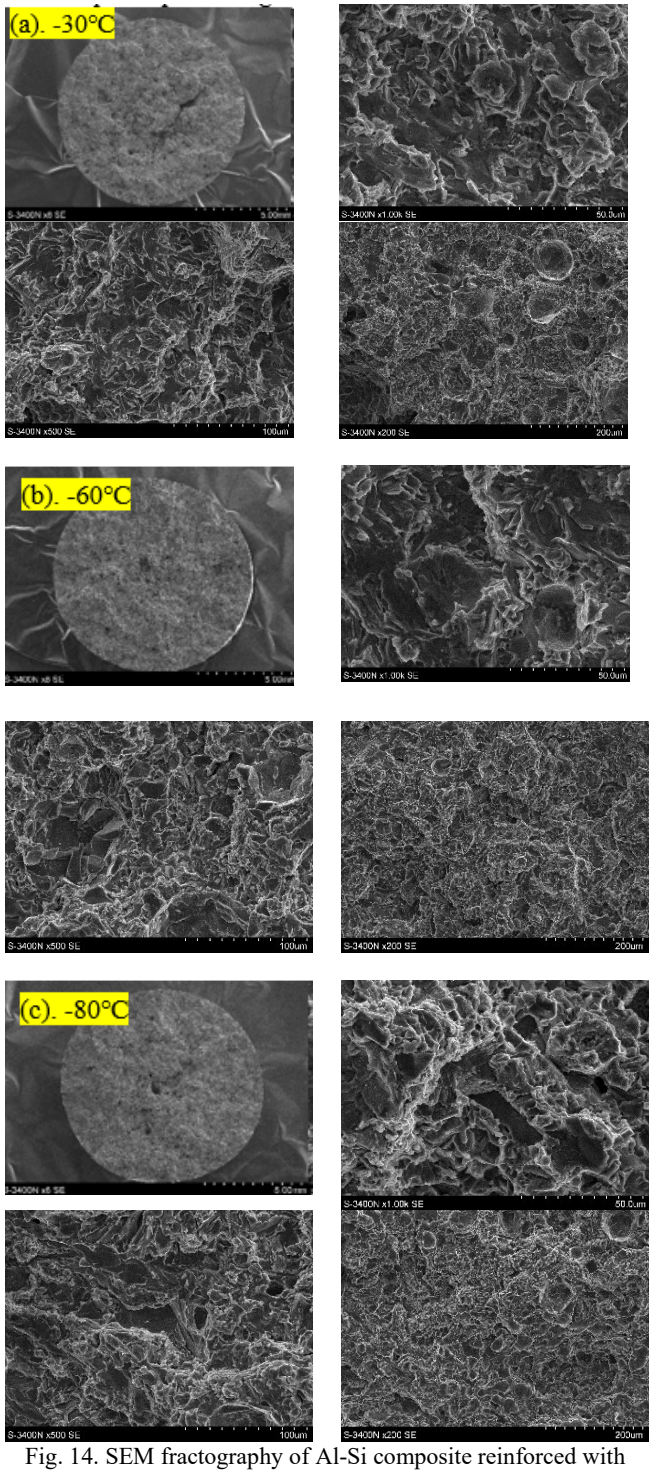

Fig. 14. SEM fractography of Al-Si composite reinforced with SiC, showing fracture surfaces of specimens tested at different temperatures: -30°C (a), -60°C (b), and -80°C (c); scale bars: 5 mm, 50 µm, 100 µm, and 200 µm (from left to right)

4. Conclusions

This study investigated the low-temperature mechanical properties and fracture behaviour of the EN AC-AlSi12CuNiMg alloy and its SiC-reinforced composite under tensile loading at temperatures ranging from room temperature, -30°C, -60°C and -80°C. The key insights from this research work are summarized below.

- The results demonstrated a significant increase in ultimate tensile strength (UTS) for both materials as the temperature decreased, with the alloy showing a 38.6% improvement at -80°C and the composite a 15.3% increase offer valuable performance benchmarks for applications where strength enhancement is prioritized, such as cryogenic support structure. However, the materials exhibited limited ductility, with elongation values below 5%, indicating brittle fracture behaviour. This poses a concern for applications requiring toughness, as stress concentrations near eutectic Si and intermetallic phases promote failure, necessitating smooth design transitions.
- Fractographic analysis revealed cleavage facets, radial cracks, and intergranular textures, confirming brittle failure driven by stress concentrators such as eutectic Si particles and intermetallic phases. The composite also showed SiC-matrix debonding and porosity, which further compromised ductility and load transfer efficiency. These findings underscore the critical role of microstructural features, including particle distribution and interfacial bonding, in governing fracture behaviour at low temperatures. The study highlights the trade-off between strength and ductility in cryogenic environments, emphasizing the need for careful material selection and microstructural optimization for low-temperature applications. Strategies to mitigate stress concentrations and enhance interfacial bonding, particularly in the SiC-reinforced composite, are essential to improve fracture resistance. Future work should employ advanced characterization techniques, such as electron backscatter diffraction (EBSD) and energy-dispersive X-ray spectroscopy (EDS), to further elucidate crack propagation mechanisms and microstructural influences.
- In conclusion, while the EN AC-AlSi12CuNiMg alloy and its SiC-reinforced composite exhibit enhanced strength at low-temperatures, their brittle fracture behaviour limits their use in applications requiring ductility. Optimizing microstructure and interfacial properties is crucial for improving their performance in demanding low-temperature environments. These insights contribute to the development of advanced aluminium-based materials for structural applications under extreme conditions.

Acknowledgements

This research was funded by Silesian University of Technology, young scientist grant number 11/030/BKM24/1202.

Authors would like to appreciate significant contributions from dr hab. inż. Anna Dolata, prof. PŚ and dr hab. inż. Maciej Dyzia for manufacturing the studied specimens.

References

[1] Yan, J.-B. & Xie, J. (2017). Experimental studies on mechanical properties of steel reinforcements under cryogenic temperatures. *Construction and Building Materials*. 151, 661–672. DOI.org/10.1016/j.conbuildmat.2017.06.123.

[2] Dang, W., Zhang, W., Yi, Y., Huang, S., He, H. & Zhang, J. (2024). Influence of retrogression temperature and time on microstructure, mechanical properties and corrosion behaviours of cryogenically-deformed 7A85 aluminium alloy. *Transactions of Nonferrous Metals Society of China*. 34(2), 392-407. DOI.org/10.1016/S1003-6326(23)66406-4.

[3] Barthélémy, H., Weber, M. & Barbier, F. (2017). Hydrogen storage: Recent improvements and industrial perspectives. *International Journal of Hydrogen Energy*. 42(11), 7254-7262. DOI:10.1016/j.ijhydene.2016.03.178.

[4] Mekonnin, A. S. & Wacławiak, K. (2025). Investigation of material properties under cryogenic conditions: a review. Zeszyty Naukowe. Organizacja i Zarządzanie/Politechnika Śląska. DOI.org/10.29119/1641-3466.2025.216.22.

[5] Luo, D., Liu, M., Jiang, X., Yu, Y., Zhang, Z., Feng, X. & Lai, C. (2022). Effect of yttrium-based rare earth on inclusions and cryogenic temperature impact properties of offshore engineering steel. *Crystals*. 12(3), 305, 1-16. DOI.org/10.3390/cryst12030305.

[6] Mekonnin, A.S., Wacławiak, K., Humayun, M., Zhang, S. & Ullah, H. (2025). Hydrogen storage technology, and its challenges: a review. *Catalysts.* 15(3), 260, 1-38. DOI.org/10.3390/catal15030260.

[7] Sápi, Z. & Butler R. (2020). Properties of cryogenic and low temperature composite materials–A review. *Cryogenics*. 111, 103190, 1-18. DOI.org/10.1016/j.cryogenics.2020.103190.

[8] Qiu, Y., Yang, H., Tong, L. & Wang, L. (2021). Research progress of cryogenic materials for storage and transportation of liquid hydrogen. *Metals*. 11(7), 1101, 1-13. DOI.org/10.3390/met11071101.

[9] de Rosso, E., dos Santos, C.A. & Garcia A. (2022). Microstructure, hardness, tensile strength, and sliding wear of hypoeutectic Al–Si cast alloys with small Cr additions and Fe-impurity content. *Advanced Engineering Materials*. 24(8), 2001552, 1-13. DOI.org/10.1002/adem.202001552.

[10] Jin, M., Lee, B., Yoo, J., Jo, Y. & Lee S. (2024). Cryogenic deformation behaviour of aluminium alloy 6061-T6. *Metals and Materials International.* 30(6), 1492-1504. DOI: 10.1007/s12540-023-01594-5.

[11] Kahrıman, F. & Zeren, M. (2017). Microstructural and mechanical characterization of Al-0.80 Mg-0.85 Si-0.3 Zr alloy. *Archives of Foundry Engineering*. 17(4), 73-78. DOI: 10.1515/afe-2017-0133.

[12] Nguyen, T.D., Singh, C., Kim, Y.S., Han, J.H., Lee, D.H., Lee, K., Harjo, S. & Lee, S.Y. (2024). Mechanical properties of base metal and heat-affected zone in friction-stir-welded AA6061-T6 at ultra-low temperature of 20 K. *Journal of Materials Research and Technology*. 31, 1547-1556. DOI.org/10.1016/j.jmrt.2024.06.165.

[13] Hirsch, J. (2014). Recent development in aluminium for automotive applications. *Transactions of Nonferrous Metals Society of China*. 24(7), 1995-2002. https://doi.org/10.1016/S1003-6326(14)63305-7.

[14] Verstraete, D., Hendrick, P., Pilidis, P. & Ramsden, K. (2010). Hydrogen fuel tanks for subsonic transport aircraft, *International Journal of Hydrogen Energy*. 35(20), 11085-11098. DOI.org/10.1016/j.ijhydene.2010.06.060.

[15] Yan, J.-B., Kong, G. & Zhang L. (2023). Low-temperature tensile behaviours of 6061-T6 aluminium alloy: tests, analysis, and numerical simulation. *Structures*. 56, 105054, 1-17. DOI.org/10.1016/j.istruc.2023.105054.

[16] Xi, R., Xie, J. & Yan, J.-B. (2024). Evaluations of low-temperature mechanical properties and full-range constitutive models of AA 5083-H112/6061-T6. *Construction and Building Materials*. 411, 134520, 1-14. DOI.org/10.1016/j.conbuildmat.2023.134520.

[17] Kumar, M., Sotirov, N., Grabner, F., Schneider, R. & Mozdzen, G. (2017). Cryogenic forming behaviour of AW-6016-T4 sheet. *Transactions of Nonferrous Metals Society of China*. 27(6), 1257-1263. DOI: 10.1016/S1003-6326(17)60146-8.

[18] Gruber, B., Grabner, F., Falkinger, G., Schökel, A., Spieckermann, F., Uggowitzer, P. J., & Pogatscher, S. (2020). Room temperature recovery of cryogenically deformed aluminium alloys. *Materials & design*. 193, 108819, 1-13. DOI.org/10.1016/j.matdes.2020.108819.

[19] Park, D.-H., Choi, S.-W., Kim, J.-H. & Lee, J.-M. (2015). Cryogenic mechanical behaviour of 5000-and 6000-series aluminium alloys: Issues on application to offshore plants. *Cryogenics*. 68, 44-58. DOI.org/10.1016/j.cryogenics.2015.02.001.

[20] Tiwari, S., Biswas, P., Mandal, N. & Roy, S. (2025). Effect of SiC Particle Size and content on the mechanical and tribological properties of porous Si3N4-SiC Composites fabricated following a facile low-temperature processing route. *Ceramics International*. 51(14), 19508-19523. DOI.org/10.1016/j.ceramint.2025.02.126.

[21] Jayashree, P., Gowrishankar, M., Sharma, S., Shetty, R., Hiremath, P. & Shettar, M. (2021). The effect of SiC content in aluminum-based metal matrix composites on the microstructure and mechanical properties of welded joints. *Journal of Materials Research and Technology.* 12, 2325-2339. DOI.org/10.1016/j.jmrt.2021.04.015.

[22] Lijay, K.J., Selvam, J.D.R., Dinaharan, I. & Vijay S. (2016). Microstructure and mechanical properties characterization of AA6061/TiC aluminum matrix composites synthesized by in situ reaction of silicon carbide and potassium fluotitanate. *Transactions of Nonferrous Metals Society of China.* 26(7), 1791-1800. DOI.org/10.1016/S1003-6326(16)64255-3.

[23] Kurzawa, A. & Kaczmar, J. (2017). Bending strength of EN AC-44200–Al_2O_3 composites at elevated temperatures. *Archives of Foundry Engineering*. 17(1), 103-108. DOI: 10.1515/afe-2017-0019.

[24] Kurzawa, A. & Kaczmar, J. (2017). Impact strength of composite materials based on EN AC-44200 matrix reinforced with Al2O3 particles. *Archives of Foundry Engineering*. 17(3), 73-78. DOI: 10.1515/afe-2017-0094.

[25] Sahin, Y. (2003). Preparation and some properties of SiC particle reinforced aluminium alloy composites. *Materials &*

design. 24(8), 671-679. DOI.org/10.1016/S0261-3069(03)00156-0.
[26] Wysocki, J., Grabian, J. & Przetakiewicz, W. (2007). Continuous drive friction welding of cast AlSi/SiC (p) metal matrix composites. *Archives of Foundry Engineering*. 7(1), 47-52.
[27] Ozden, S., Ekici, R. & Nair, F. (2006). Investigation of impact behaviour of aluminium based SiC particle reinforced metal–matrix composites. *Composites Part A: Applied Science and Manufacturing*. 38(2), 484-494. DOI:10.1016/j.compositesa.2006.02.026.
[28] Aybarc, U., Dispinar, D. & Seydibeyoglu, M.O. (2018). Aluminum metal matrix composites with SiC, Al_2O_3 and graphene–review. *Archives of Foundry Engineering.* 18(2), 5-10. DOI. 10.24425/122493.
[29] Li, R., Pan, Z., Zeng, Q. & Xiaoli, Y. (2022). Influence of the interface of carbon nanotube-reinforced aluminium matrix composites on the mechanical properties–a review. *Archives of Foundry Engineering*. 22(1), 23-36. DOI 10.24425/afe.2022.140213.
[30] Ozben, T., Kilickap, E. & Cakır, O. (2008). Investigation of mechanical and machinability properties of SiC particle reinforced Al-MMC. *Journal of Materials Processing Technology.* 198(13), 220-225. DOI:10.1016/j.jmatprotec.2007.06.082.
[31] Pawar, P. & Utpat, A.A. (2014). Development of aluminium based silicon carbide particulate metal matrix composite for spur gear. *Procedia materials science*. 6, 1150-1156. DOI: 10.1016/j.mspro.2014.07.187.
[32] Sampath, D., Akid, R. & Morana, R. (2018). Estimation of crack initiation stress and local fracture toughness of Ni-alloys 945X (UNS N09946) and 718 (UNS N07718) under hydrogen environment via fracture surface topography analysis. *Engineering Fracture Mechanics*. 191, 324-343. DOI.org/10.1016/j.engfracmech.2017.12.010.
[33] Macek, W., Branco, R., Podulka, P., Kopec, M., Zhu, S.-P. & Costa, J.D. (2023). A brief note on entire fracture surface topography parameters for 18Ni300 maraging steel produced by LB-PBF after LCF. *Engineering Failure Analysis*. 153, 107541, 1-17. DOI.org/10.1016/j.engfailanal.2023.107541.
[34] Kobayashi T. & Shockey, D.A. (2010). Fracture surface topography analysis (FRASTA)—development, accomplishments, and future applications. *Engineering fracture mechanics.* 77(12), 2370-2384. DOI.org/10.1016/j.engfracmech.2010.05.016.
[35] Sirata, G.G., Wacławiak, K. & Dyzia, M. (2022). Mechanical and microstructural characterization of aluminium alloy, EN AC-Al Si12CuNiMg. *Archives of Foundry Engineering*. 22(3), 34-40. DOI.10.24425/afe.2022.140234.
[36] Sirata, G., Wacławiak, K. & Dolata, A. (2024). Microstructure and Mechanical Properties of the EN AC-AlSi12CuNiMg Alloy and AlSi Composite Reinforced with SiC Particles. *Archives of Foundry Engineering*. 24(2), 50-59. DOI.10.24425/afe.2024.149271.
[37] Liu, Y., Jia, L., Wang, W., Jin, Z. & Zhang, H. (2023). Reinforcing Al matrix composites by novel intermetallic/SiC interface and transition structure. *Journal of Materials Research and Technology.* 26, 164-175. DOI.org/10.1016/j.jmrt.2023.07.166.
[38] Gruber, B., Weißensteiner, I., Kremmer, T., Grabner, F., Falkinger, G., Schökel, A., Spieckermann, F., Schäublin, R., Uggowitzer, P. & Pogatscher, S. (2020). Mechanism of low temperature deformation in aluminium alloys. *Materials Science and Engineering: A*. 795, 139935, 1-11. DOI.org/10.1016/j.msea.2020.139935.
[39] Wendt, U. (2021). Engineering materials and their properties. In K.-H. Grote & H. Hefazi (Eds.), *Springer Handbook of Mechanical Engineering* (2nd ed., pp. 233–292). Springer Cham. https://doi.org/10.1007/978-3-030-47035-7_8.
[40] Park D.-Y. & Niewczas, M. (2018). Plastic deformation of Al and AA5754 between 4.2 K and 295 K. *Materials Science and Engineering: A*. 491(1-2), 88-102. https://doi.org/10.1016/j.msea.2008.01.065.